Electronic Supplementary Information

Dual acid-responsive bola-type supramolecular vesicles for efficient intracellular anticancer drug delivery

Guangping Sun,[a‡] Zhimei He,[c‡] Min Hao,[a] Minzan Zuo,[a] Zuqiang Xu,[a] Xiao-Yu Hu,*[a,b] Jun-Jie Zhu,*[c] and Leyong Wang*[a,d]

[a] *Key Laboratory of Mesoscopic Chemistry of MOE, Jiangsu Key Laboratory of Advanced Organic Materials, School of Chemistry and Chemical Engineering, Nanjing University, Nanjing, 210023, China. E-mail: lywang@nju.edu.cn*

[b] *Applied Chemistry Department, College of Material Science and Technology, Nanjing University of Aeronautics and Astronautics, Nanjing, 211100, China. E-mail: huxy@nuaa.edu.cn*

[c] *State Key Laboratory of Analytical Chemistry for Life Science, Collaborative Innovation Center of Chemistry for Life Science, School of Chemistry and Chemical Engineering, Nanjing University, Nanjing 210023, China. E-mail: jjzhu@nju.edu.cn*

[d] *School of Petrochemical Engineering, Changzhou University, Changzhou, 213164, China.*

‡ Guangping Sun and Zhimei He contributed equally to this work.

Table of Contents

1. General information and experimental procedure S2

2. Synthesis of host **WP5**, guest **G**, model guest molecule $\mathbf{G_M}$, and control guest molecule **G'** S5

3. Job plot of complex **WP5⊃G** S19

4. Determination of the association constant (K_a) for **WP5⊃$\mathbf{G_M}$** complex S20

5. Tyndall effects of free DOX, **WP5⊃G** vesicles, and DOX-loaded **WP5⊃G** vesicles S21

6. Determination of the best molar ratio of **WP5** and **G** leading to aggregation S21

7. Critical aggregation concentration (CAC) determination of **WP5⊃G** S22

8. Zeta-potentials of the aggregates formed by **WP5⊃G** S23

9. DLS and TEM data of **WP5⊃G'** vesicles S23

10. The extended length of the **G** S23

11. References S24

1. General information and experimental procedure

1) General information:

All reactions were performed in air atmosphere unless otherwise stated. The commercially available reagents and solvents were either employed as purchased or dried according to procedures described in the literature. Column chromatography was performed with silica gel (200 – 300 mesh) produced by Qingdao Marine Chemical Factory, Qingdao (China). All yields were given as isolated yields. NMR spectra were recorded on a Bruker DPX 400 MHz spectrometer with internal standard tetramethylsilane (TMS) and solvent signals as internal references at room temperature, and the chemical shifts (δ) were expressed in ppm and *J* values were given in Hz. High-resolution electrospray ionization mass spectra (HR-ESI-MS) were recorded on an Agilent 6540Q-TOF LCMS equipped with an electrospray ionization (ESI) probe operating in the positive-ion mode with direct infusion. Low-resolution electrospray ionization mass spectra (LR-ESI-MS) were obtained on Finnigan Mat TSQ 7000 instruments. Transmission electron microscope (TEM) investigations were carried out on a JEM-2100 instrument. Dynamic light scattering (DLS) measurements were carried out on a Brookhaven BI-9000AT system (Brookhaven Instruments Corporation, USA), using a 200-mW polarized laser source (λ = 514 nm). Zeta-potential measurements were performed at 25 ℃ on a Zetasizer Nano Z apparatus (Malvern Instruments Ltd., UK) using the Smoluchowski model for the calculation of the Zeta-potential from the measured electrophoretic mobility. The UV-Vis absorption spectra were measured on a Perkin Elmer Lambda 35 UV-Vis Spectrometer. The confocal laser scanning microscopy (CLSM) investigations were carried out on a Zeiss LSM 710 instrument. The excitation and emission spectra were recorded on a Hitachi F-7000 Fluorescence Spectrometer.

2) Experimental procedure:

Fabrication of the DOX-loaded vesicles. DOX-loaded vesicles were prepared as follows: a certain amount of DOX (after being desalted by TEA) was added to a solution containing **WP5** and **G**. The ultimate concentrations of DOX, **G**, and **WP5** were 0.07, 0.4, and 0.14 mM, respectively. After standing overnight, the prepared DOX-loaded **WP5⊃G** vesicles were purified by dialysis (molecular weight cutoff 10000) in distilled water for several times until the water outside the dialysis tube exhibited negligible DOX fluorescence.

The DOX encapsulation efficiency was calculated by equation (1):

$$\text{Encapsulation efficiency (\%)} = (m_{DOX\text{-}loaded}/m_{DOX}) \times 100 \quad (1)$$

where $m_{DOX\text{-}loaded}$ and m_{DOX} are mass of DOX encapsulated into the vesicles and mass of DOX added, respectively. The mass of DOX was measured by a fluorescence spectrophotometer at 560 nm.

The DOX loading efficiency was calculated based on equation (2):

$$\text{Loading efficiency (\%)} = (m_{DOX\text{-}loaded}/m_{DOX\text{-}loaded+vesicles}) \times 100 \quad (2)$$

where $m_{DOX\text{-}loaded}$ and $m_{DOX\text{-}loaded+vesicles}$ are mass of DOX encapsulated into the vesicles and mass of DOX-loaded vesicles, respectively.

Acid-responsive behavior of the drug-loaded vesicles. 0.05 M tris-HCl buffer solution (pH = 7.4) and 0.1 M citrate buffer solution (pH = 5.0 and 6.0) were used as drug release media to simulate the normal physiological condition and the intracellular condition of tumor cells. In a typical release experiment, 8.4 mL of DOX-loaded **WP5⊃G** vesicles was added into 1.6 mL of appropriate release medium at 37 ℃. At selected time intervals, 2 mL of the release media was taken out for measuring the released DOX concentrations by the fluorescence technique, and then was returned to the original release media. A nearly 100% release of DOX from DOX-loaded **WP5⊃G** vesicles was obtained by adding Triton X-100 to the vesicular solution.

***In vitro* cytocompatibility and cytotoxicity assay.** The relative *in vitro* cytocompatibility of **G**, **WP5⊃G** vesicles, **G'**, **WP5⊃G'** vesicles, and free DOX against NIH 3T3 normal cells, and the relative *in vitro* cytotoxicity of free DOX, DOX-loaded **WP5⊃G** vesicles and DOX-loaded **WP5⊃G'** vesicles against MCF-7 and U87MG cancer cells were assessed by using the MTT assay (NIH 3T3, MCF-7, and U87MG cell lines were supplied by KeyGen Biotech Co. Ltd, Nanjing, China). Firstly, the cells were seeded in 96-well plates at a density of 2×10^4 cells per well in 200 μL of DMEM containing 10% fetal bovine serum (Gibco), 50 $U \cdot mL^{-1}$ penicillin, and 50 $U \cdot mL^{-1}$ streptomycin (Hyclone), and cultured in 5% CO_2 at 37 ℃ for 24 h. Then, the original medium was removed and 200 μL of fresh culture medium containing different concentrations of **G**, **WP5⊃G** vesicles, **G'**, **WP5⊃G'** vesicles, and free DOX (for NIH 3T3 normal cells) or free DOX, DOX-loaded **WP5⊃G** vesicles, and DOX-loaded **WP5⊃G'** vesicles (for MCF-7 and U87MG cancer cells) was added into each well, and the cells were further incubated for 24 h.

Subsequently, 200 μL of MTT solution (0.5 mg/mL) was added into each well and incubated for

another 4 h. After that, the medium containing MTT was removed, and dimethyl sulfoxide (DMSO, 150 μL) was added to each well to dissolve the MTT formazan crystals. Finally, the plates were shaken for 30 min, and the absorbance of formazan product was measured at 490 nm by a microplate reader (Thermo Scientific). Untreated cells in medium were used as the blank control. All experiments were carried out with four replicates. The biocompatibility and cytotoxicity were expressed as the percentage of the cell viability relative to the blank control.

Cellular uptake and intracellular localization observed by CLSM. The cellular uptake and intracellular localization of DOX were examined in MCF-7 and U87MG cancer cells. Briefly, MCF-7 and U87MG cells were plated onto glass-bottomed Petri dishes in 400 μL of complete DMEM culture medium at a density of 1×10^5 cells for 24 h before treatment. Then cells were incubated with DOX-loaded **WP5⊃G** vesicles solution (equivalent to 2 μM DOX) for 1 h. Then, the culture medium was removed and cells were washed with PBS thrice. Then, LysoTracker Green (2 μM, Cell Signaling Technology, USA) was added to the medium for 30 min at 37℃ to label lysosomes. Next, the cells were washed three times with PBS after being fixed by 400 μL paraformaldehyde for 10 min. Subsequently, DAPI (Cell Signaling Technology, USA) was added to the medium for 15 min to stain nuclei. Finally, the cells were washed three times with PBS and investigated by confocal laser scanning microscopy (LSM710, CarlZeiss). The fluorescence characteristics of DOX-loaded **WP5⊃G** vesicles were used to directly monitor the localization of DOX without utilizing additional dye.

Flow cytometric analysis. MCF-7 and U87MG cells were seeded in six-well plates at a density of 2×10^5 cells per well in 1.2 mL of complete DMEM and cultured at 37 ℃ in a 5% CO_2 atmosphere for 24 h. After treating with free DOX (2 μM), DOX-loaded **WP5⊃G** vesicles ([DOX] = 2 μM) and DOX-loaded **WP5⊃G'** vesicles ([DOX] = 2 μM) for 8 h at 37 ℃, the cells were then rinsed two times with cold PBS. After trypsinizing, the cells were washed with cold PBS, centrifuged, and dispersed in 500 μL cold PBS. And then, the cells were subjected to flow cytometric analysis using a BD FACSCalibur flow cytometer, and 1×10^4 cells were tested for each sample.

2. Synthesis of host WP5, guest G, model guest molecule G_M, and control guest molecule G'

1) Synthesis of host WP5

WP5 was synthesized and purified according to previously reported procedures (Scheme S1).[S1-S6]

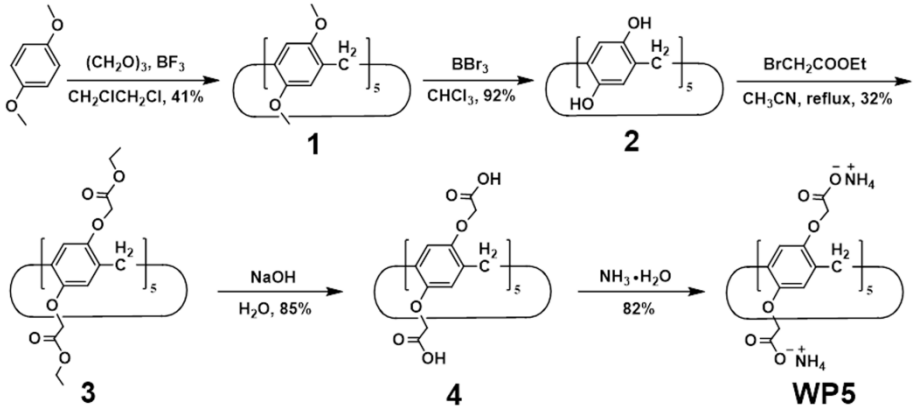

Scheme S1. Synthesis route of host **WP5.**

2) Synthesis of guest G

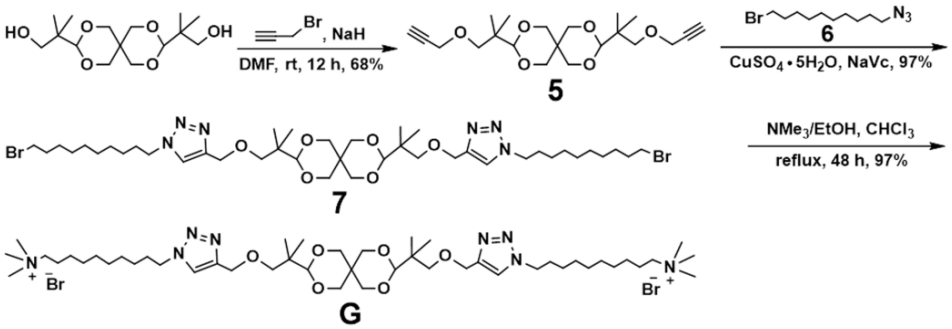

Scheme S2. Synthesis route of guest **G.**

Synthesis of compound 5

3,9-bis(1,1-dimethyl-2-hydroxyethyl)-2,4,8,10-tetraoxaspiro[5.5]undecane (0.97 g, 3.18 mmol), and sodium hydride (0.76 g, 19.00 mmol) was dissolved in DMF (25 mL) and stirred for 1 h. Then, the solution of 3-bromo-1-propyne (1.52 g, 12.78 mmol, in 15 mL DMF) was added dropwise into the above mixture during 15 min. The mixture was further stirred overnight and quenched with water (20 mL). And the mixture was extracted with chloroform (3 × 200 mL) and the organic phase were dried over Na_2SO_4, filtered, and concentrated. The crude product was purified by silica gel chromatography using dichloromethane/ethyl acetate (100:1, *v/v*) as the eluent to afford

compound **5** as a white solid (0.82 g, 2.16 mmol, 68%). ^{1}H NMR (400 MHz, $CDCl_3$, 298 K) δ (ppm) = 4.50 (dd, *J* = 11.2, 2.4 Hz, 2H), 4.30 (s, 2H), 4.10 (d, *J* = 2.4 Hz, 4H), 3.57 – 3.49 (m, 4H), 3.34 – 3.30 (m, 6H), 2.40 (t, *J* = 2.4 Hz, 2H), 0.94 (d, *J* = 4.4 Hz, 12H). ^{13}C NMR (100 MHz, $CDCl_3$, 298 K) δ (ppm) = 105.1, 80.2, 75.8, 73.9, 70.6, 70.2, 58.6, 39.1, 32.6, 19.54, 19.50. LR-ESI-MS: m/z $[M + Na]^+$ calcd for $[C_{21}H_{32}O_6Na]^+$ 403.21, found 403.25. HR-ESI-MS: m/z $[M + Na]^+$ calcd for $[C_{21}H_{32}O_6Na]^+$ 403.2091, found 403.2083.

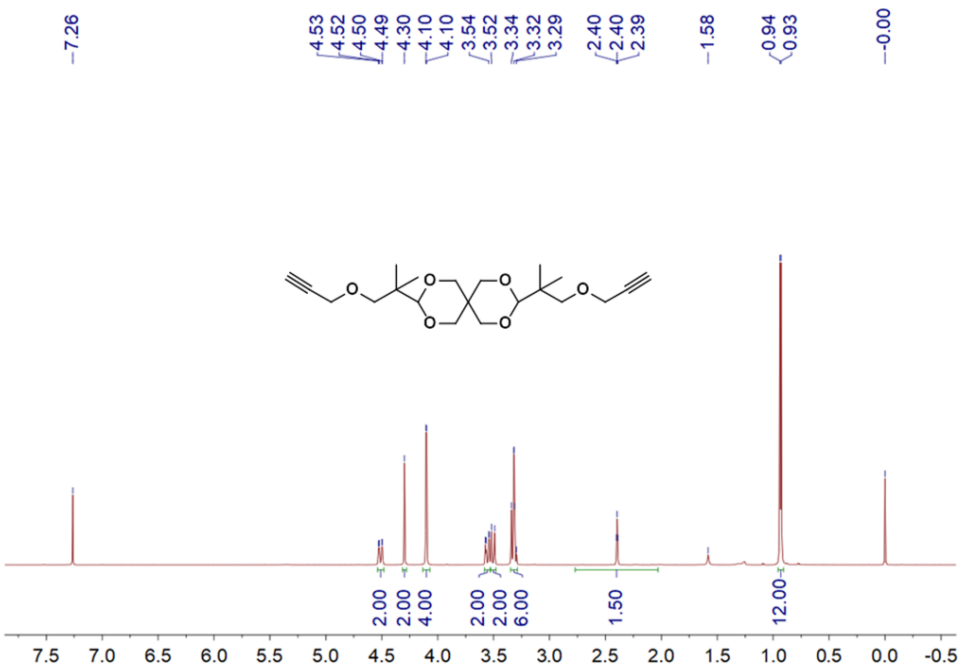

Fig. S1 ^{1}H NMR spectrum (400 MHz, $CDCl_3$, 298 K) of compound **5**.

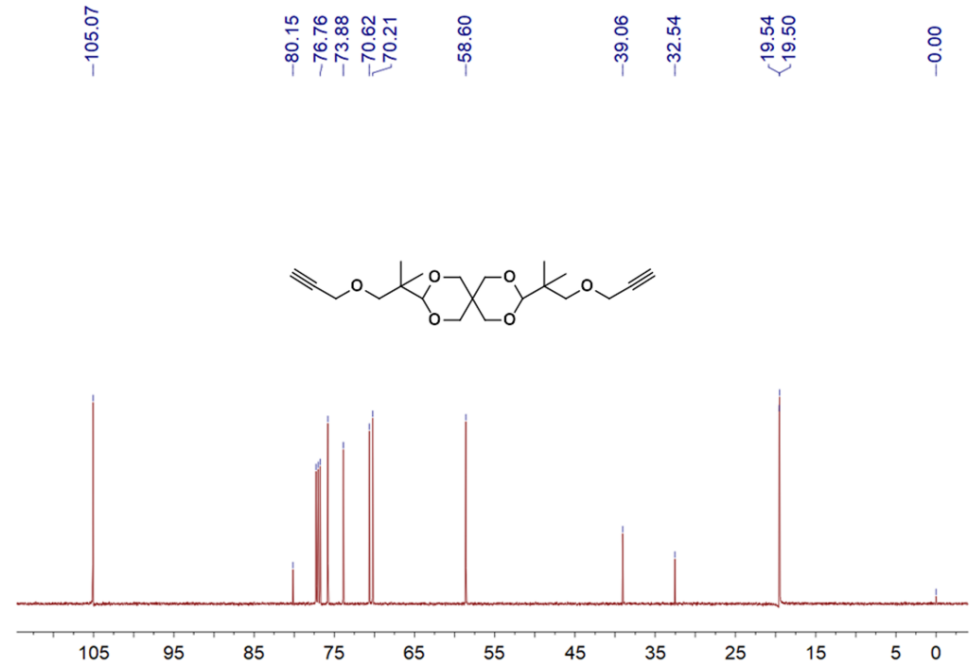

Fig. S2 ^{13}C NMR spectrum (100 MHz, $CDCl_3$, 298 K) of compound **5**.

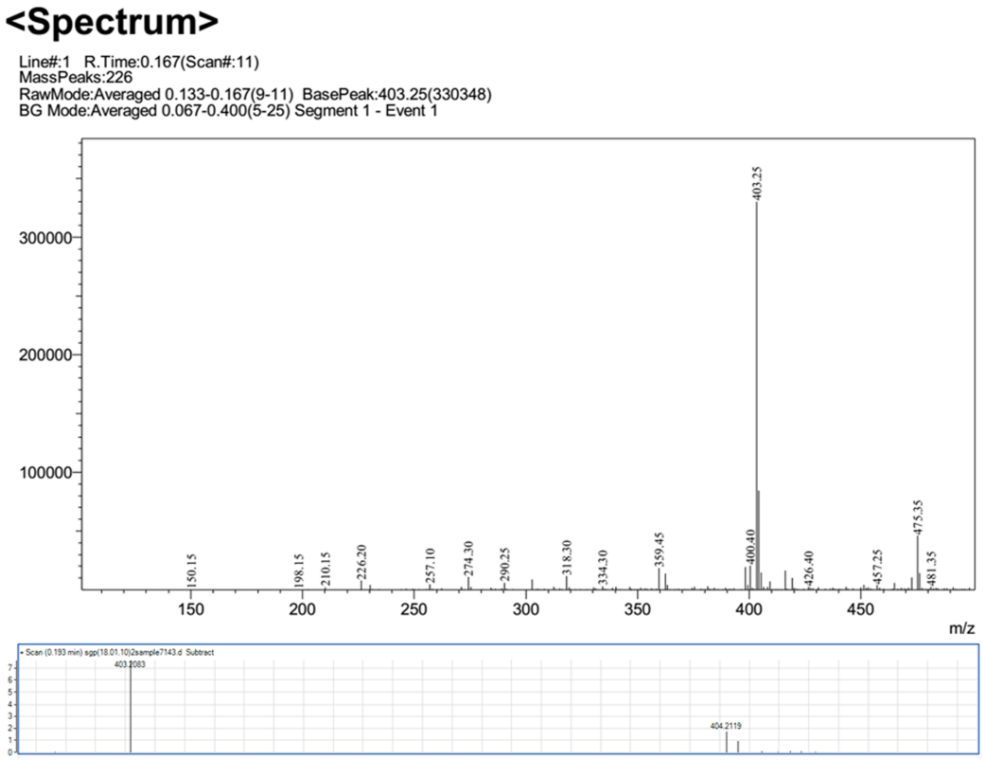

Fig. S3 LR-ESI-MS and HR-ESI-MS spectra of compound **5**.

Synthesis of compound 6

1,10-dibromodecane (5.7 g, 19 mmol) and TBAB (0.3 g, 0.93 mmol) were dissolved in DMF (100 mL). NaN_3 (1.23 g, 19 mmol) was added into the mixture over 30 min and stirred at room

temperature for 72 h. Water (1000 mL) was added to quench the reaction. The aqueous layer was extracted with dichloromethane (3 × 200 mL), and the organic layer was washed by water (1000 mL) and saturated brine (500 mL), respectively. Finally, the organic layer was dried over Na_2SO_4, filtered, and concentrated to afford compound **6** as colorless oil (3.62 g, 13.87 mmol, 73%). ^{1}H NMR (400 MHz, $CDCl_3$, 298 K) δ (ppm) = 3.41 (t, *J* = 6.8 Hz, 2H), 3.26 (t, *J* = 7.2 Hz, 2H), 1.89 – 1.82 (m, 2H), 1.63 – 1.56 (m, 2H), 1.44 – 1.30 (m, 12H). ^{13}C NMR (100 MHz, $CDCl_3$, 298 K) δ (ppm) = 51.5, 34.1, 32.8, 29.4, 29.3, 29.1, 28.8, 28.7, 28.2, 26.7.

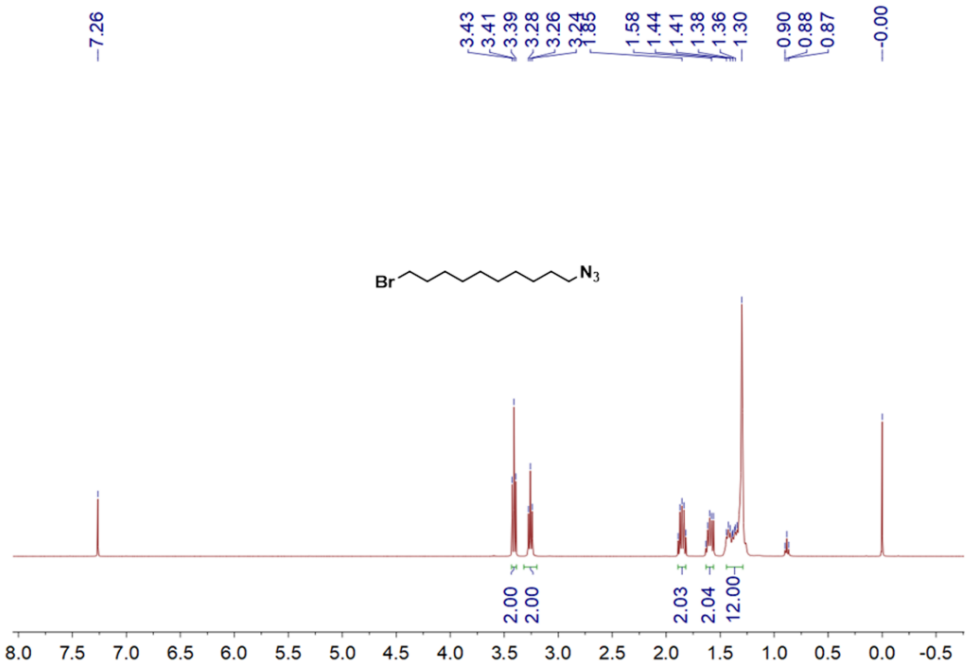

Fig. S4 ^{1}H NMR spectrum (400 MHz, $CDCl_3$, 298 K) of compound **6**.

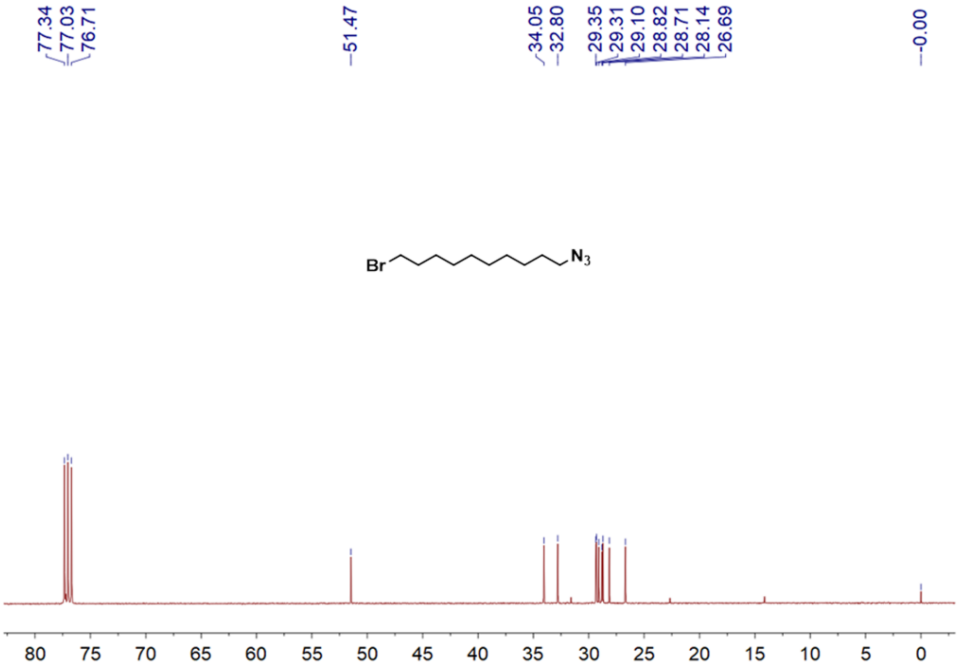

Fig. S5 ^{13}C NMR spectrum (100 MHz, $CDCl_3$, 298 K) of compound **6**.

Synthesis of compound 7

Compound **5** (0.11 g, 0.32 mmol), copper sulfate pentahydrate (30 mg, 0.12 mmol) and sodium ascorbate (80 mg, 0.57 mmol) were added to a solution of compound **6** (0.33 g, 1.22 mmol) dissolved in dichloromethane (10 mL), then H_2O (10 mL) was added to the above mixture. The mixture was stirred under Argon atmosphere in room temperature for 48 h. The reaction mixture was diluted with dichloromethane (10 mL) and washed with water (3 × 10 mL). The organic phase was dried over magnesium sulfate and filtered. The solvent was removed under reduced pressure. Purification via anhydrous diethyl ether afforded compound **7** as a white solid (0.28 g, 0.31 mmol, 97%). ^{1}H NMR (400 MHz, $CDCl_3$, 298 K) δ (ppm) = 7.50 (s, 2H), 4.61 (s, 4H), 4.48 (d, *J* = 10.8 Hz, 2H), 4.35 (t, *J* = 6.8 Hz, 4H), 4.29 (s, 2H), 3.55 – 3.46 (m, 4H), 3.41 (t, *J* = 6.8 Hz, 2H), 3.34 – 3.29 (m, 4H), 3.24 – 1.29 (m, 36H), 0.92 (d, *J* = 2 .8 Hz, 12H). ^{13}C NMR (100 MHz, $CDCl_3$, 298 K) δ (ppm) = 145.7, 122.0, 105.1, 76.2, 70.6, 70.2, 65.1, 50.3, 39.2, 34.0, 32.8, 32.5, 30.3, 29.3, 29.2, 28.9, 28.7, 28.1, 26.4, 19.53, 19.52. LR-ESI-MS: m/z $[M + H]^+$ calcd for $[C_{41}H_{73}Br_2N_6O_6]^+$ 903.40, 905.39, 907.39, found 903.35, 905.35, 907.25, m/z $[M + Na]^+$ calcd for $[C_{41}H_{72}Br_2N_6O_6Na]^+$ 925.38, 927.38, 929.37, found 925.35, 927.30, 929.25. HR-ESI-MS: m/z $[M + H]^+$ calcd for $[C_{41}H_{73}Br_2N_6O_6]^+$ 903.3953, 905.3932, 907.3912, found 903.3937, 905.3922,

907.3916, m/z [M + Na]$^+$ calcd for [$C_{41}H_{72}Br_2N_6O_6Na$]$^+$ 925.3772, 927.3752, 929.3731, found 925.3761, 927.3749, 929.3738.

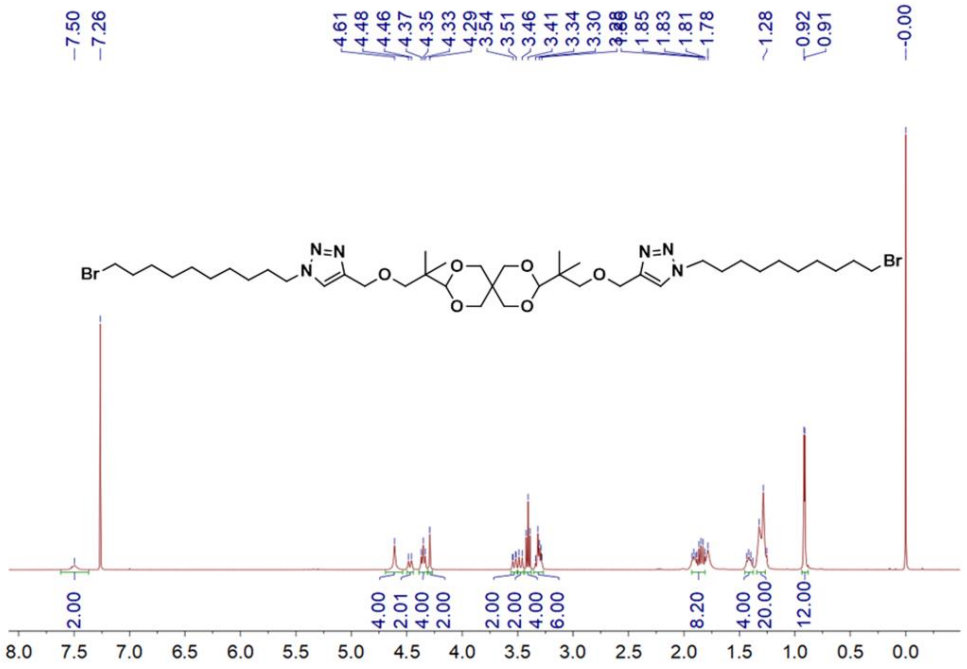

Fig. S6 ^{1}H NMR spectrum (400 MHz, $CDCl_3$, 298 K) of compound **7**.

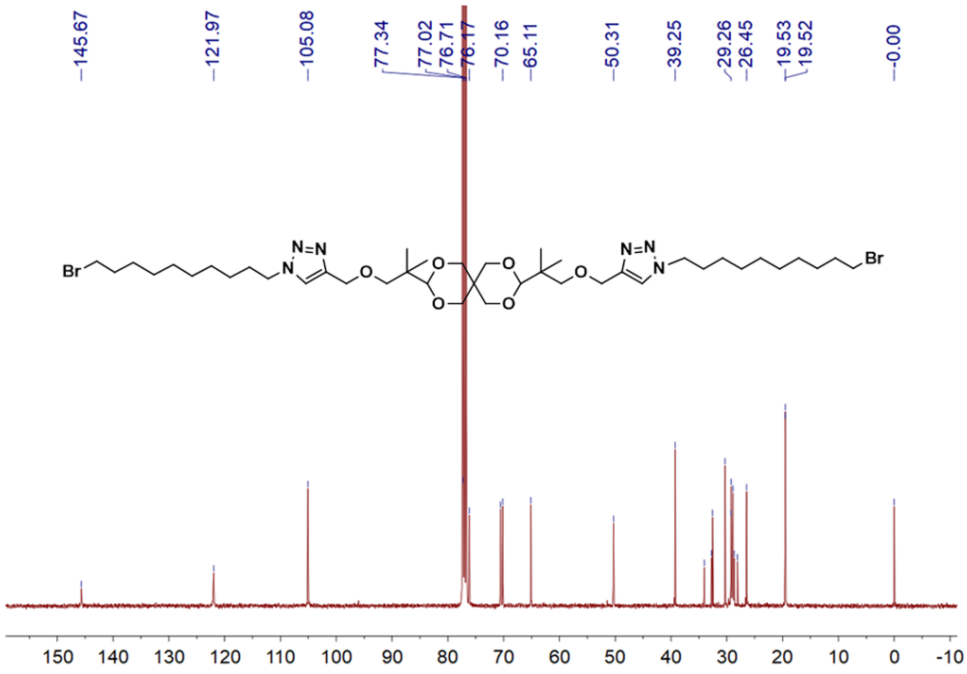

Fig. S7 ^{13}C NMR spectrum (100 MHz, $CDCl_3$, 298 K) of compound **7**.

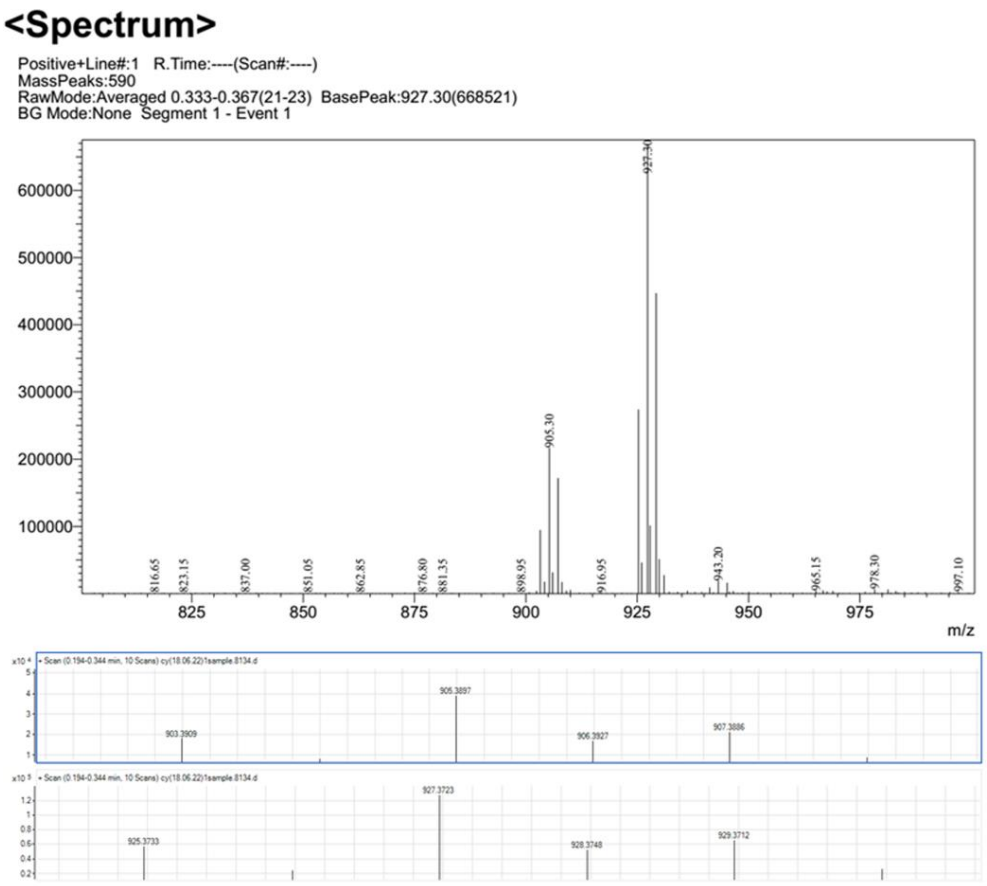

Fig. S8 LR-ESI-MS and HR-ESI-MS spectra of compound **7**.

Synthesis of compound G

Compound **7** (0.28 g, 0.32 mmol) and trimethylamine/ethanol solution (1 mL) were dissolved in chloroform (15 mL) and refluxed overnight. The mixture were concentrated under reduced pressure and washed by anhydrous ether to give **G** as a white solid (0.32 g, 0.31 mmol, 97%). ^{1}H NMR (400 MHz, D_2O, 298 K) δ (ppm) = 7.92 (s, 2H), 4.55 – 4.46 (m, 4H), 4.33 (t, *J* = 6.8 Hz, 4H), 4.25 (s, 2H), 4.11 (d, *J* = 10.8 Hz, 2H), 3.47 – 3.40 (m, 4H), 3.32 (d, *J* = 11.6 Hz, 2H), 3.23 – 3.17 (m, 8H), 3.00 (s, 18H), 1.83 – 1.76 (m, 4H), 1.68 – 1.64 (m, 4H), 1.22 – 1.09 (m, 24H), 0.78 (d, *J* = 8 Hz, 12H). ^{13}C NMR (100 MHz, D_2O, 298 K) δ (ppm) = 144.1, 124.9, 105.1, 74.8, 69.8, 69.4, 66.7, 63.1, 55.2, 52.8, 50.3, 44.7, 38.4, 32.2, 29.4, 28.5, 28.4, 28.2, 28.0, 25.5, 22.3, 19.2, 18.7. LR-ESI-MS: m/z $[M - 2Br]^{2+}$ calcd for $[C_{47}H_{90}N_8O_6]^{2+}$ 431.35, found 431.35. HR-ESI-MS: m/z $[M - 2Br]^{2+}$ calcd for $[C_{47}H_{90}N_8O_6]^{2+}$ 431.3486, found 431.3497.

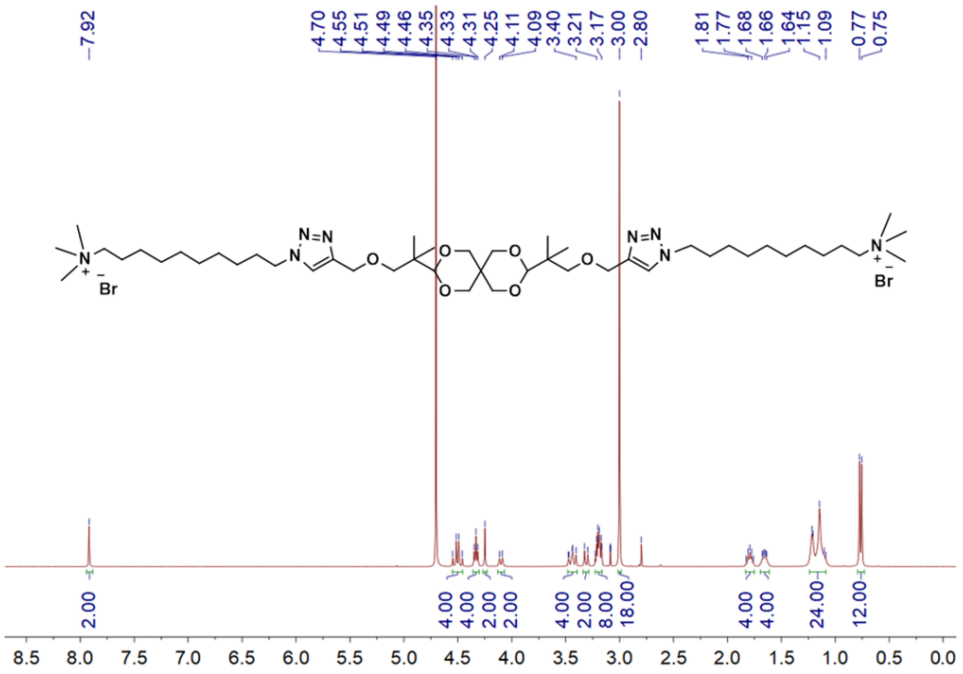

Fig. S9 ^{1}H NMR spectrum (400 MHz, D_2O, 298 K) of **G**.

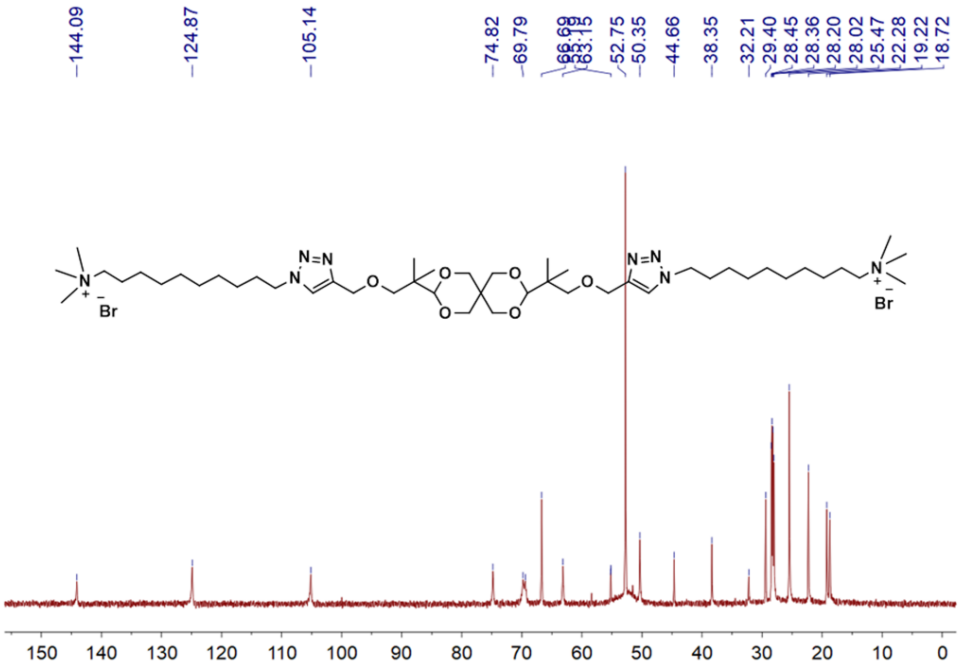

Fig. S10 ^{13}C NMR spectrum (100 MHz, D_2O, 298 K) of **G**.

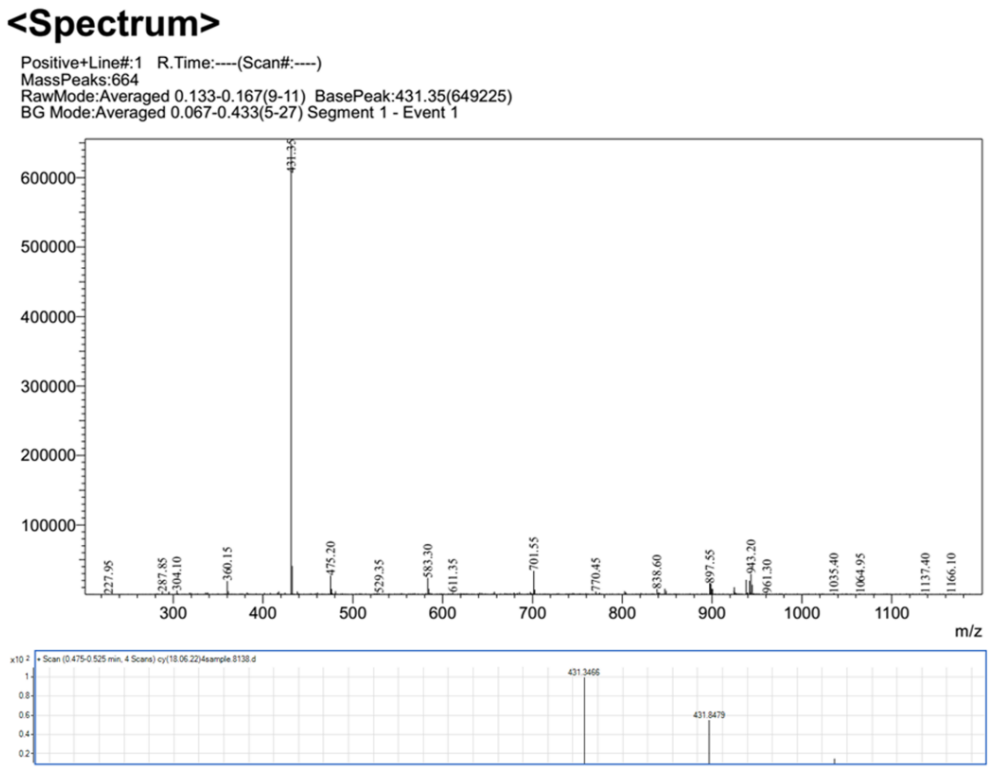

Fig. S11 LR-ESI-MS and HR-ESI-MS spectra of **G**.

3) Synthesis of model guest molecule G_M

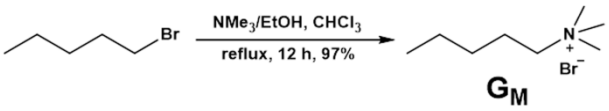

Scheme S3. Synthesis of model guest molecule $\mathbf{G_M}$.

Bromopentane (0.048 g, 0.32 mmol) and trimethylamine/ethanol solution (1 mL) were dissolved in chloroform (15 mL) and refluxed overnight. The mixture were concentrated under reduced pressure and washed by anhydrous ether to give $\mathbf{G_M}$ as a white solid (0.064 g, 0.31 mmol, 98%). ^{1}H NMR (400 MHz, D_2O, 298 K) δ (ppm) = 3.32 – 3.28 (m, 2H), 3.10 (s, 9H), 1.82 – 1.74 (m, 2H), 1.38 – 1.32 (m, 4H), 0.90 (t, J = 6.8 Hz, 2H).

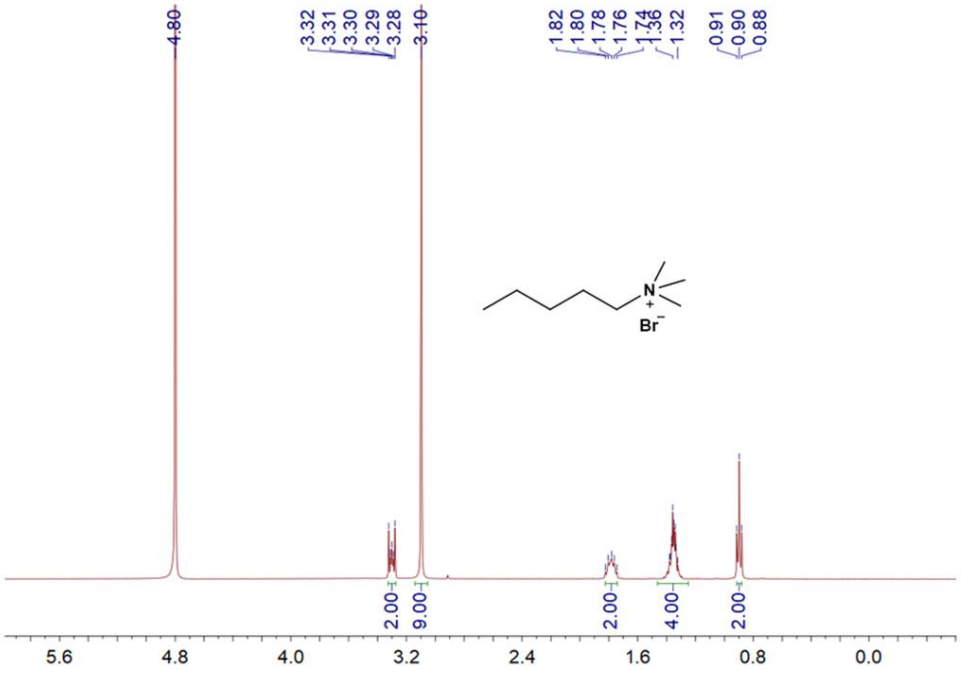

Fig. S12 ^{1}H NMR spectrum (400 MHz, D_2O, 298 K) of compound $\mathbf{G_M}$.

4) Synthesis of control guest molecule G'

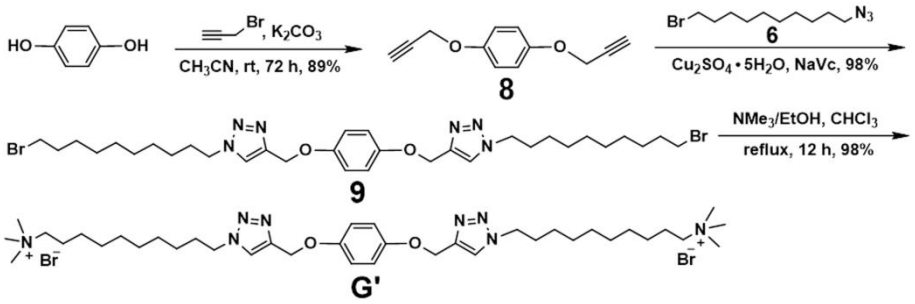

Scheme S4. Synthesis of control guest molecule **G'**.

Synthesis of compound 8

Hydroquinone (11.0 g, 100 mmol) and K_2CO_3 (27.6 g, 200 mmol) were added to a solution of propargyl bromide (47.5 g, 200 mmol) in CH_3CN (180 mL). The mixture was heated in a two-necked flask under Argon atmosphere at reflux for 72 h. The solid was filtered off and the solvent was removed. The residue was dissolved in dichloromethane and washed with water five times. The organic layer was dried over anhydrous Na_2SO_4 and evaporated to afford the crude product, which was purified by silica gel chromatography (dichloromethane/petroleum ether, v/v = 1:2 to yield a white solid compound **8** (16.554 g, 89 %).^{1}H NMR (400 MHz, $CDCl_3$, 298 K) δ (ppm) = 6.93 (s, 4H), 4.65 (d, *J* = 2.4 Hz, 4H), 2.51 (t, *J* = 2.0 Hz, 2H).

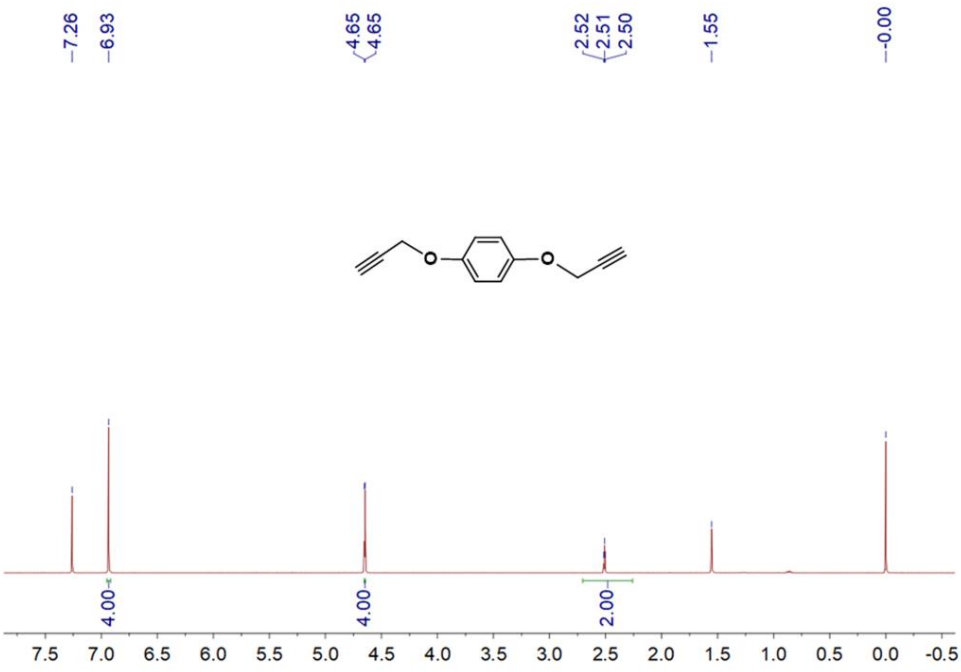

Fig. S13 ^{1}H NMR spectrum (400 MHz, $CDCl_3$, 298 K) of compound **8**.

Synthesis of compound 9

Compound **8** (0.5 g, 2.68 mmol), copper sulfate pentahydrate (0.19 g, 1.01 mmol), and sodium ascorbate (0.67 g, 4.77 mmol) were added to the dichloromethane (30 mL) solution of compound **6** (2.76 g, 10.22 mmol). Then H_2O (30 mL) was added to the above mixture. The mixture was stirred under argon atmosphere in room temperature for 48 h. The reaction mixture was diluted with dichloromethane (20 mL) and washed with water (3 × 50 mL). The organic phase was dried over magnesium sulfate and filtered. The solvent was removed under reduced pressure. Purification via anhydrous diethyl ether afforded compound **9** as a light yellow solid (1.86 g, 2.63 mmol, 98%).^{1}H NMR (400 MHz, $CDCl_3$, 298 K) δ (ppm) = 7.67 (s, 2H), 6.93 (s, 4H), 5.16 (s, 2H), 4.36 (t, *J* = 7.2 Hz, 4H), 3.40 (t, *J* = 7.2 Hz, 4H), 1.93 – 1.81 (m, 8H), 1.43 – 1.28 (m, 20H). ^{13}C NMR (100 MHz, $CDCl_3$, 298 K) δ (ppm) =152.8, 144.6, 122.7, 115.8, 62.7, 50.5, 34.1, 32.8, 30.2, 29.3, 29.2, 28.9, 28.7, 28.1, 26.4. LR-ESI-MS: m/z $[M + H]^+$ calcd for $[C_{32}H_{51}Br_2N_6O_2]^+$ 709.24, 711.24, 713.24, found 709.15, 711.20, 713.15, m/z $[M + Na]^+$ calcd for $[C_{32}H_{50}Br_2N_6O_2Na]^+$ 731.23, 733.22, 735.22, found 731.10, 733.10, 735.00. HR-ESI-MS: m/z $[M + H]^+$ calcd for $[C_{32}H_{51}Br_2N_6O_2]^+$ 709.2435, 711.2414, 713.2394, found 709.2426, 711.2402, 713.2391, m/z $[M + Na]^+$ calcd for $[C_{32}H_{50}Br_2N_6O_2Na]^+$ 731.2254, 733.2234, 735.2213, found 731.2242, 733.2226,

735.2214.

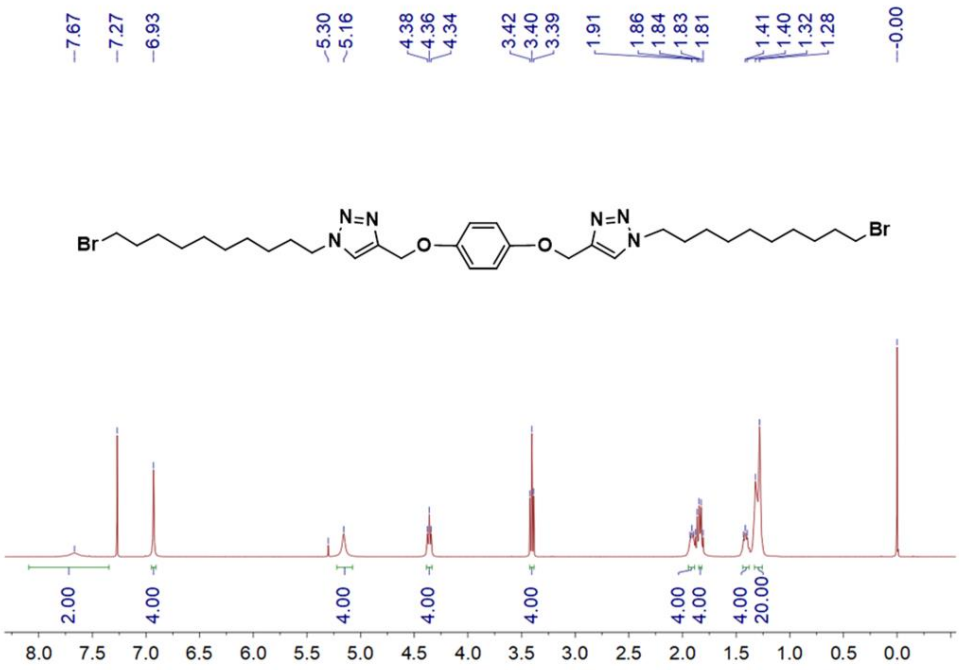

Fig. S14 ^{1}H NMR spectrum (400 MHz, $CDCl_3$, 298 K) of compound **9**.

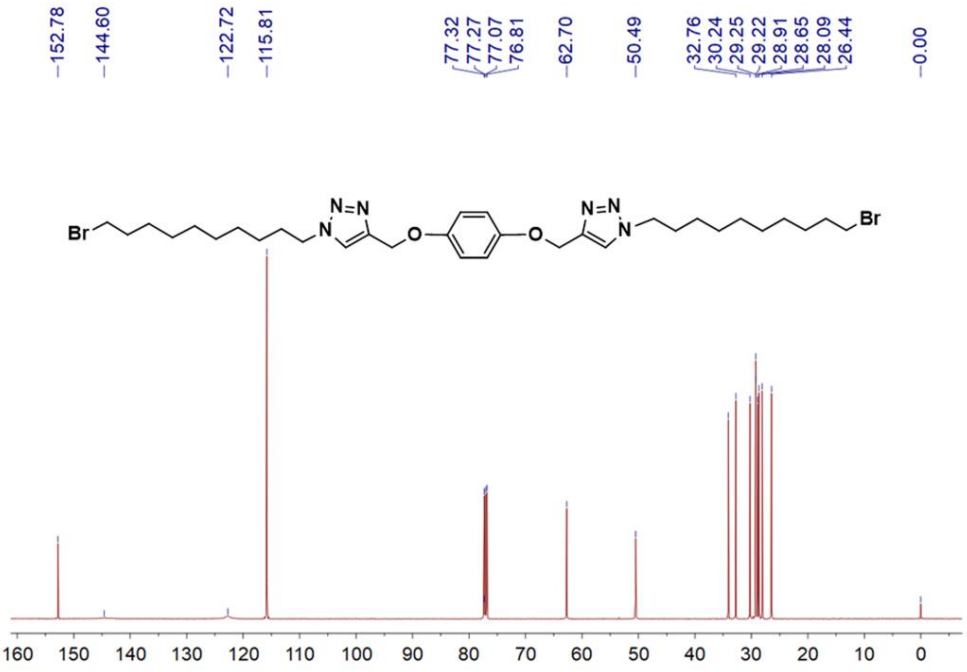

Fig. S15 ^{13}C NMR spectrum (400 MHz, $CDCl_3$, 298 K) of compound **9**.

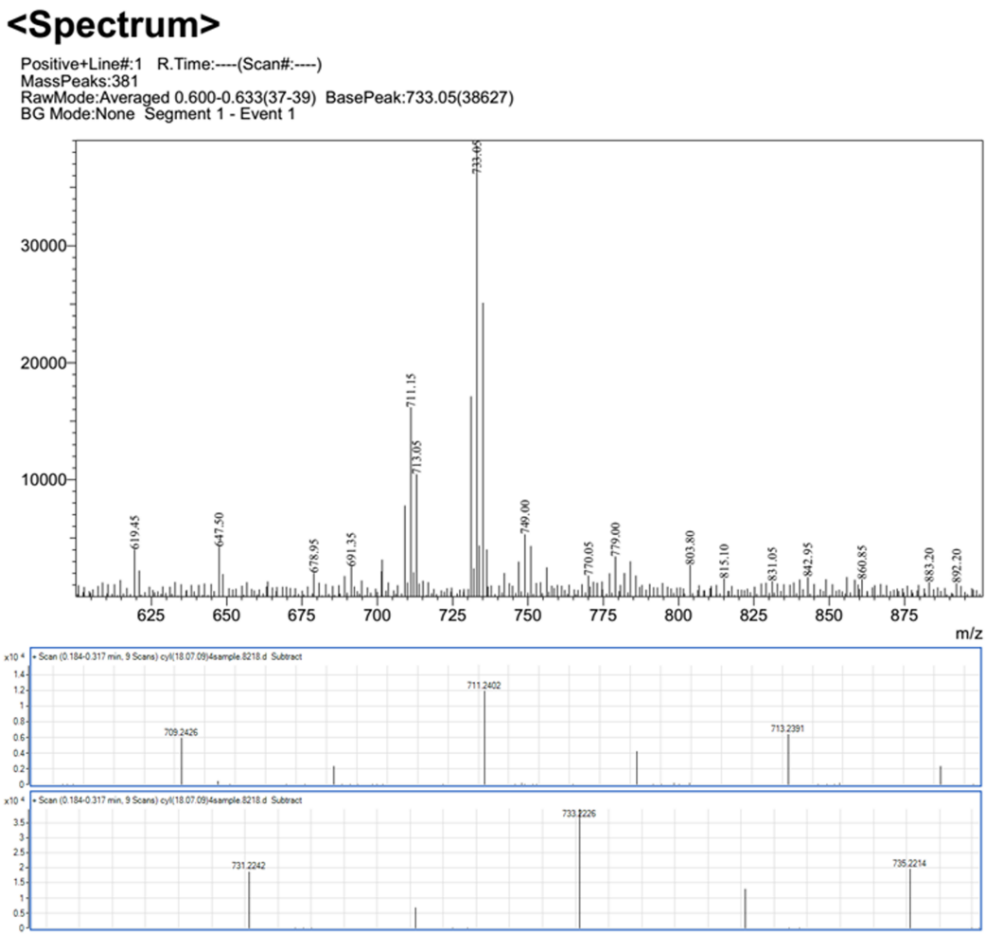

Fig. S16 LR-ESI-MS and HR-ESI-MS spectra of compound **9**.

Synthesis of compound G'

Compound **9** (0.26 g, 0.32 mmol) and trimethylamine/ethanol solution (1 mL) were dissolved in chloroform (15 mL) and refluxed overnight. The mixture were concentrated under reduced pressure and washed by anhydrous ether to give **G'** as a light yellow solid (0.26 g, 0.31 mmol, 98%). ^{1}H NMR (400 MHz, DMSO-d_6, 298 K) δ (ppm) = 8.21 (s, 2H), 6.96 (s, 4H), 5.06 (s, 4H), 4.35 (t, J = 6.8 Hz, 4H), 3.28 – 3.23 (m, 4H), 3.03 (s, 18H), 1.84 – 1.77 (m, 4H), 1.69 – 1.63 (m, 4H), 1.26 (s, 24H). ^{13}C NMR (100 MHz, DMSO-d_6, 298 K) δ (ppm) = 152.8, 143.3, 124.8, 116.1, 65.7, 62.1, 52.6, 49.8, 30.2, 29.2, 29.1, 28.9, 28.8, 26.3, 26.2, 22.5. LR-ESI-MS: m/z $[M - 2Br]^{2+}$ calcd for $[C_{38}H_{68}N_8O_2]^{2+}$ 334.27, found 334.25. HR-ESI-MS: m/z $[M - 2Br]^{2+}$ calcd for $[C_{38}H_{68}N_8O_2]^{2+}$ 334.2727, found 334.2726.

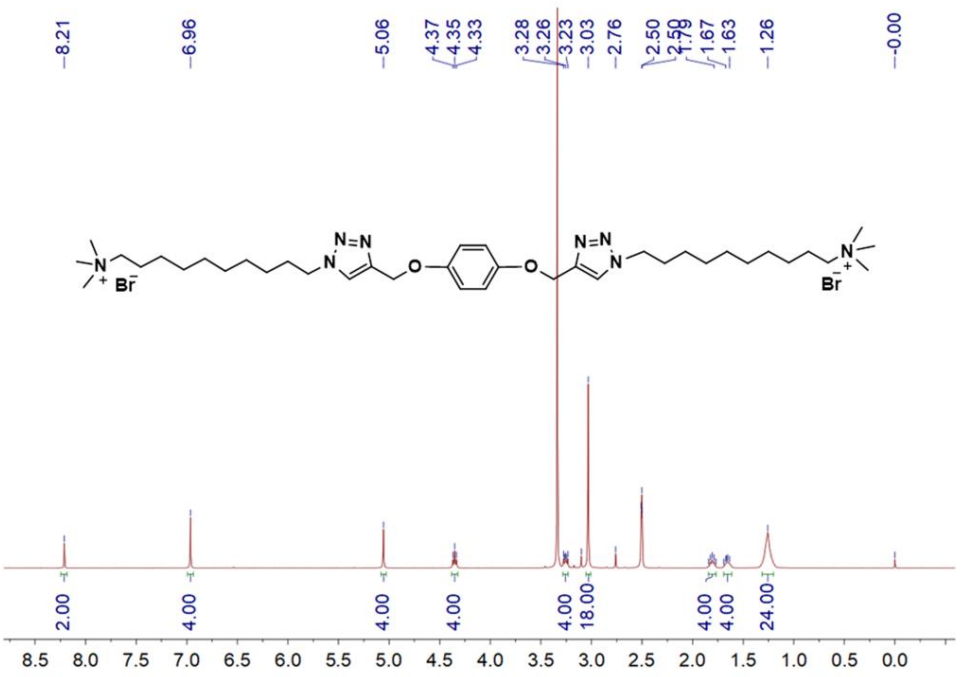

Fig. S17 ^{1}H NMR spectrum (400 MHz, DMSO-d_6, 298 K) of **G'**.

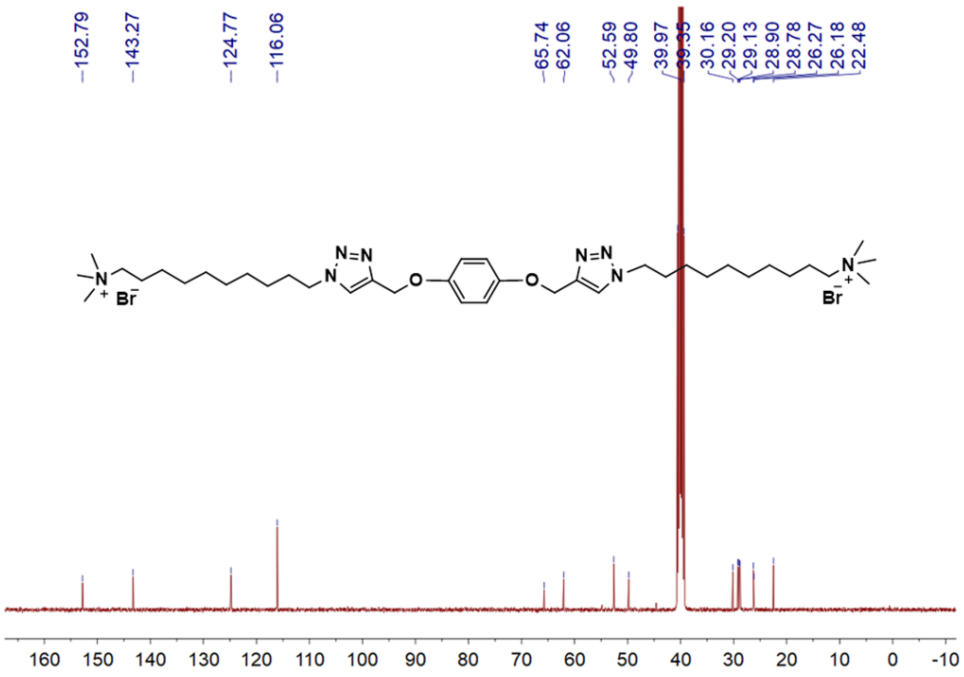

Fig. S18 ^{13}C NMR spectrum (400 MHz, DMSO-d_6, 298 K) of **G'**.

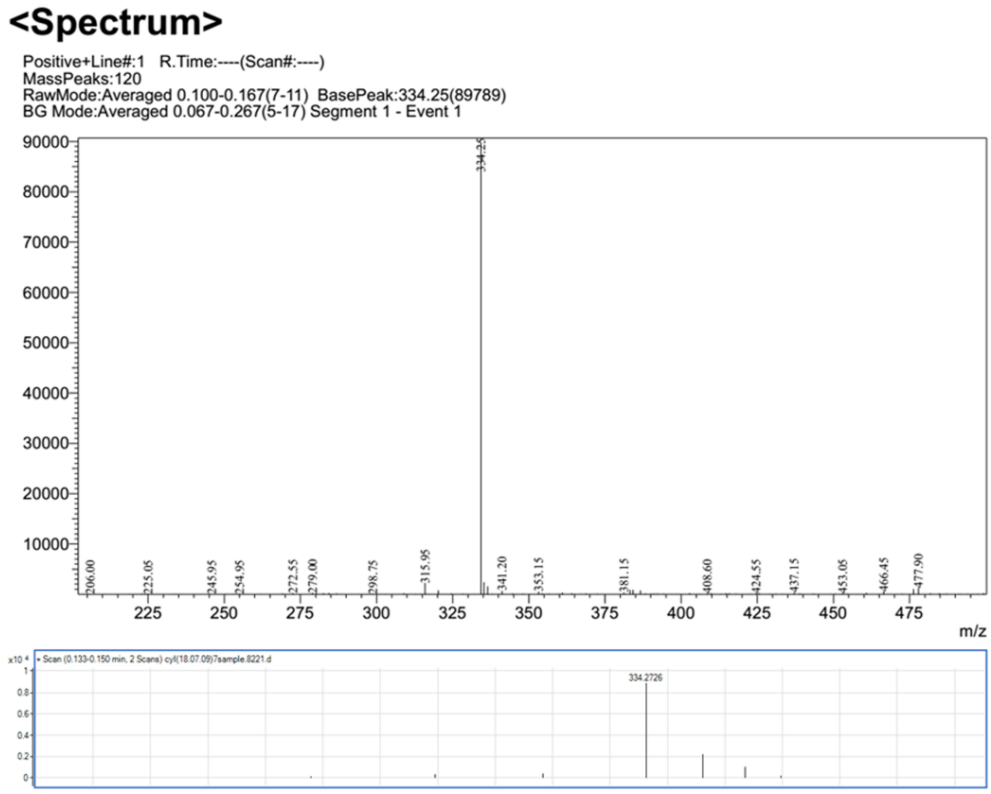

Fig. S19 LR-ESI-MS and HR-ESI-MS spectra of **G'**.

3. Job plot of complex WP5⊃G

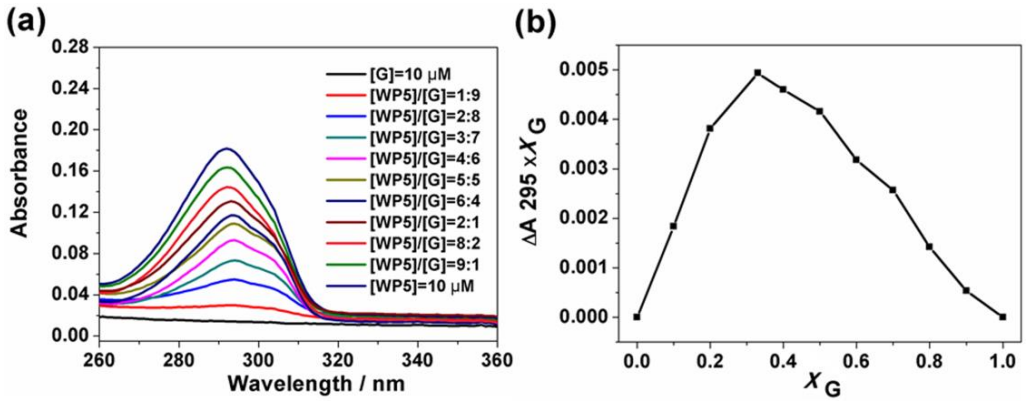

Fig. S20 (a) UV-Vis absorption spectra of complex **WP5⊃G** with different molar ratios in water while **[WP5]** + **[G]** = 10 μM. (b) Job plot of complex **WP5⊃G** showing a 2:1 stoichiometry between **WP5** and **G** by plotting the absorbance difference at 295 nm (a characteristic absorption peak of **WP5**) against the mole fraction of **WP5**.

4. Determination of the association constant (K_a) for WP5⊃G_M complex

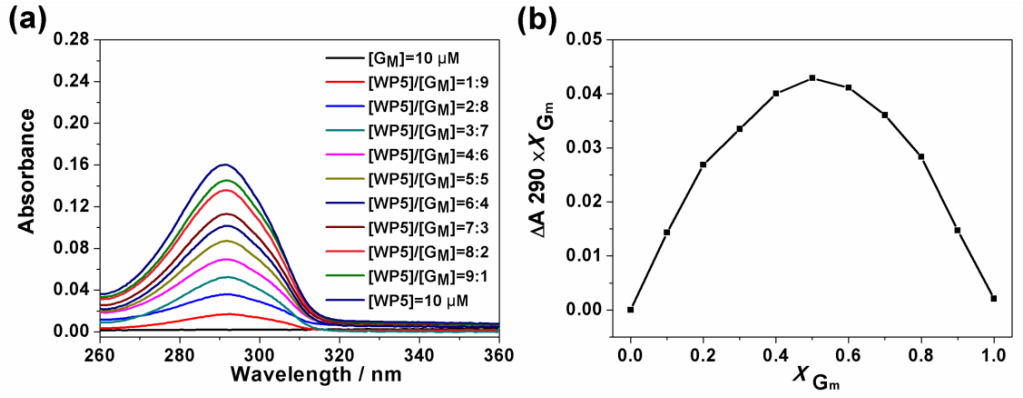

Fig. S21 (a) UV-Vis absorption spectra of complex **WP5⊃G_M** with different molar ratios in water while **[WP5]** + **[G_M]** = 10 μM. (b) Job plot of complex **WP5⊃G_M** showing a 1:1 stoichiometry between **WP5** and **G_M** by plotting the absorbance difference at 290 nm (a characteristic absorption peak of **WP5**) against the mole fraction of **WP5**.

To determine the association constant between **WP5** and **G_M**, ^{1}H NMR titrations were carried out in aqueous solution, which had a constant concentration of **G_M** (4.0 mM) and varying concentrations of **WP5**. By a non-linear curve-fitting method, the association constant between **G_M** and **WP5** was calculated. The non-linear curve-fitting was based on the following equation: $\Delta\delta = (\Delta\delta_\infty/[G]_0)(0.5[H]_0+0.5([G]_0+1/K_a)-(0.5([H]_0^2+(2[H]_0(1/K_a-[G]_0))+(1/K_a+[G]_0)^2)^{0.5}))$. Where $\Delta\delta$ is the chemical shift change of H_b on **G_M** at $[H]_0$, $\Delta\delta_\infty$ is the chemical shift change of H_b when the guest is completely complexed, $[G]_0$ is the fixed initial concentration of the guest (**G_M**), and $[H]_0$ is the varying concentrations of **WP5**.

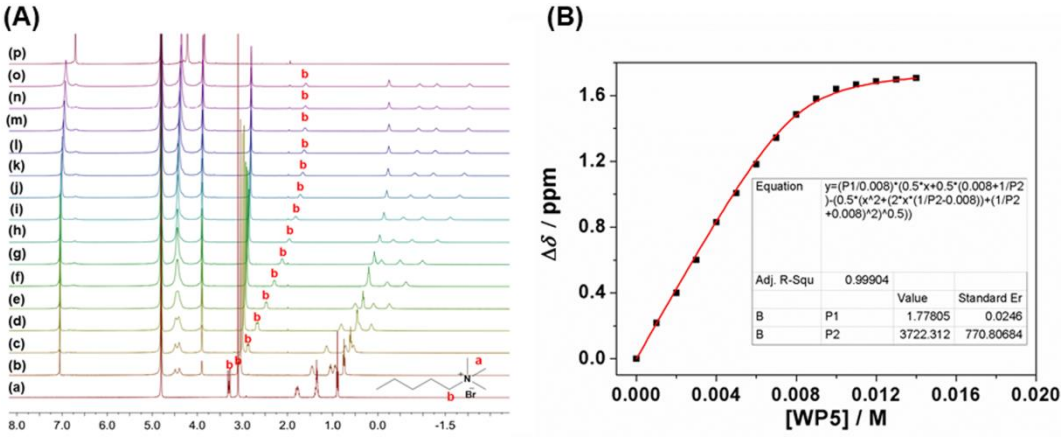

Fig. S22 (A) ^{1}H NMR spectra (400 MHz, D_2O, 298 K) of **G_M** at a constant concentration of 8.0 mM with different

concentrations of **WP5** (mM): (a) 0.0, (b) 1.0, (c) 2.0, (d) 3.0, (e) 4.0, (f) 5.0, (g) 6.0, (h) 7.0, (i) 8.0, (j) 9.0, (k) 10.0, (l) 11.0, (m) 12.0, (n) 13.0, (o) 14.0 and (p) **WP5** (8.0 mM). (B) The chemical shift changes of H_b on $\mathbf{G_M}$ upon addition of **WP5**. The red solid line was obtained from the non-linear curve-fitting using. The association constant (K_a) of **WP5** and $\mathbf{G_M}$ was estimated to be about (3.72 ±0.77) $\times 10^3$ M^{-1}.

5. Tyndall effects of free DOX, WP5⊃G vesicles, and DOX-loaded WP5⊃G vesicles

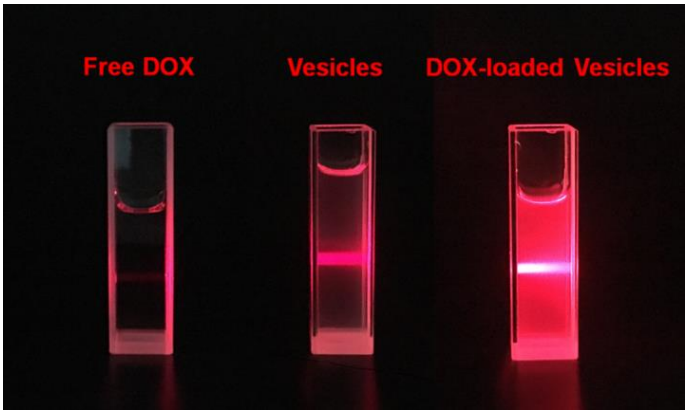

Fig. S23 Tyndall effects of free DOX, **WP5⊃G** vesicles, and DOX-loaded **WP5⊃G** vesicles

6. Determination of the best molar ratio of WP5 and G leading to aggregation

Since the addition of different amounts of **WP5** to the **G** solution could lead to obvious changes of opalescence intensity in aqueous solution, it was necessary to determine the best molar ratio between **WP5** and **G** for constructing supramolecular aggregates, which was determined by optical transmittance experiments. As shown in Fig. S24, upon gradually increasing the amount of **WP5** that was added, the optical transmittance at 500 nm firstly underwent a sharp decrease to the minimum, and thereafter an inverse increase upon further addition of **WP5**. The rapid decrease of the optical transmittance indicated that **WP5** and **G** formed a higher-order aggregate. Thus, the best molar ratio of 5:1 (**[G]/[WP5]**) for the formation of supramolecular aggregates was observed at the inflection point.

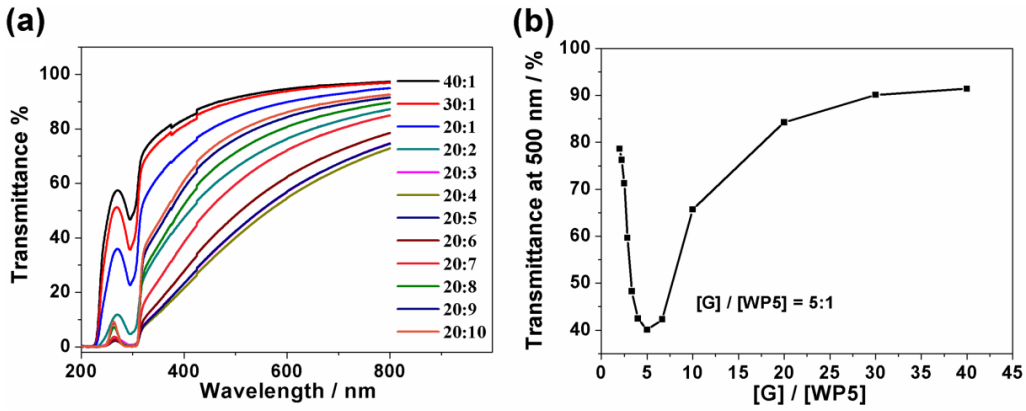

Fig. S24 (a) Optical transmittance of a mixture of **WP5** and **G** in water with a constant **G** concentration (0.4 mM) on increasing the concentration of **WP5** (0.05 – 0.5 equiv.) at 25 ℃. (b) Dependence of the relative optical transmittance at 500 nm on the **WP5** concentration with a fixed concentration of **G** (0.4 mM) at 25 ℃.

7. Critical aggregation concentration (CAC) determination of WP5⊃G

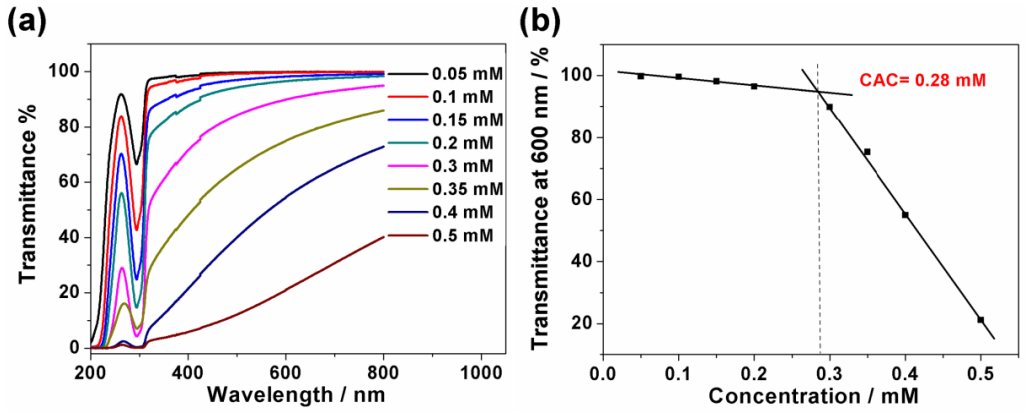

Fig. S25 Optical transmittance of a mixture of **WP5** and **G** in water with the best molar ratio of **WP5** and **G** (**[G]/[WP5]** = 5:1) on increasing the concentration of **G** (0.05 mM – 0.5 mM.) at 25 ℃.

8. Zeta-potentials of the aggregates formed by WP5⊃G

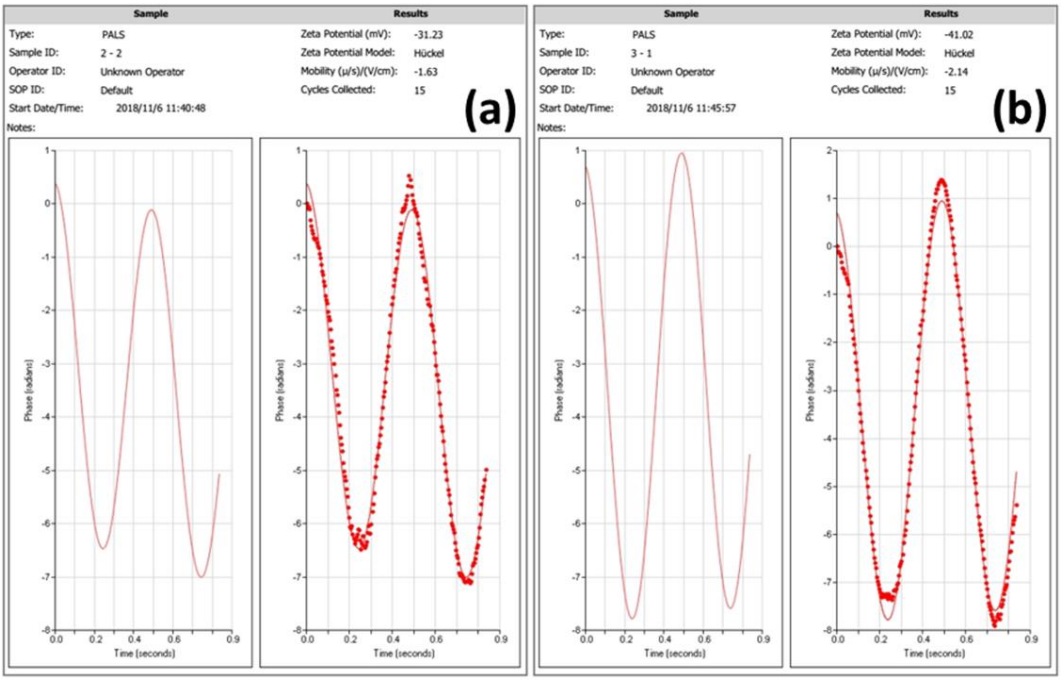

Fig. S26 Zeta-potentials of **WP5⊃G** vesicles: (a) [**G**]/[**WP5**] = 5:1; (b) [**G**]/[**WP5**] = 3:1.

9. DLS and TEM data of WP5⊃G' vesicles

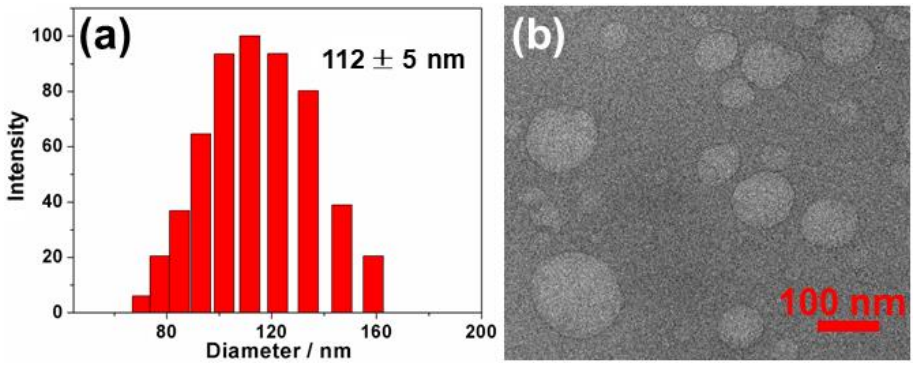

Fig. S27 (a) DLS data of **WP5⊃G'** vesicles. (b) TEM images of **WP5⊃G'** vesicles.

10. The extended length of the G

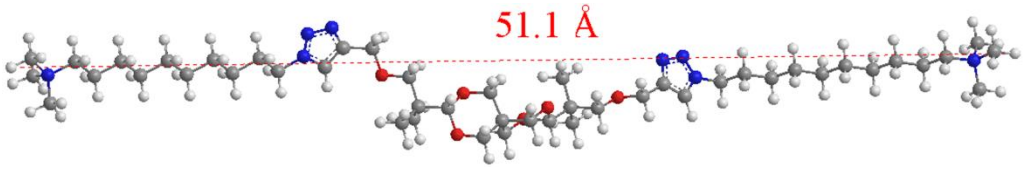

Fig. S28 The length of the **G** is calculated by MM2 method.

11. References

S1. H. Li, D.-X. Chen, Y.-L. Sun, Y. B. Zheng, L.-L. Tan, P. S. Weiss and Y.-W. Yang, *J. Am. Chem. Soc.*, 2013, **135**, 1570-1576.

S2. T. Ogoshi, S. Kanai, S. Fujinami, T.-A. Yamagishi and Y. Nakamoto, *J. Am. Chem. Soc.*, 2008, **130**, 5022-5023.

S3. D. Cao, Y. Kou, J. Liang, Z. Chen, L. Wang and H. Meier, *Angew. Chem. Int. Ed.*, 2009, **48**, 9721-9723.

S4. T. Ogoshi, M. Hashizume, T.-A. Yamagishi and Y. Nakamoto, *Chem. Commun.*, 2010, **46**, 3708-3710.

S5. Y. Ma, X. Ji, F. Xiang, X. Chi, C. Han, J. He, Z. Abliz, W. Chen and F. Huang, *Chem. Commun.*, 2011, **47**, 12340-12342.

S6. C. Li, X. Shu, J. Li, S. Chen, K. Han, M. Xu, B. Hu, Y. Yu and X. Jia, *J. Org. Chem.*, 2011, **76**, 8458-8465.